International Journal of Modern Manufacturing Technologies
ISSN 2067–3604, XV, No. 2 / 2023
https://doi.org/ 10.54684/ijmmt.2023.15.2.104

MICROSTRUCTURE AND PROPERTIES OF LASER-WELDED BUTT JOINTS OF AlSi1MgMn ALUMINIUM ALLOY

Aleksander Lisiecki[1], Wojciech Pakieła[1], Agnieszka Kurc-Lisiecka[2]

[1]Silesian University of Technology, Konarskiego 18A Str., 44-100 Gliwice, Poland
[3]WSB Merito University in Poznań, Sportowa 29 Str., 41-506 Chorzów, Poland

Corresponding author: Aleksander Lisiecki, aleksander.lisiecki@polsl.pl

Abstract: The process of autogenous laser welding of butt joints of aluminium alloy AlSi1MgMn plates with thickness of 3.0 mm was investigated. The Yb:YAG disk laser was used in the study. The aim was to determine the influence of the basic parameters of laser welding on the joint quality, fusion zone geometry, microhardness distribution across the butt joint, structure and microstructure of fusion zone (FZ) and heat affected zone (HAZ) was studied and determined. The chemical composition of the base metal was determined by spark emission spectroscopy, while the phase constituents were determined by XRD analysis. Results of the study have shown that the geometry of welds is proper without excessive imperfections. No voids were found the FZ. However, weld face of the joints are slightly convex, while the roots are slightly concave. Microscopic observations showed no discontinuities in the fusion zone of the welds. A significant decrease in hardness in the FZ was observed. The hardness in the FZ of the test joints is approx. 67÷70 $HV_{0.1}$. The fracture of the samples during tensile tests occurred in the FZ or at the boundary FZ/HAZ, and the tensile strength was ranged from 200MPa to 220MPa.

Key word: laser welding, Yb:YAG laser, aluminium alloy, AlSi1MgMn, microstructure characterisation

1. INTRODUCTION

Aluminium and its alloys belong to the group of light materials, characterized by an advantageous ratio of strength to specific weight. They also have good technological properties and are much cheaper than e.g. titanium, magnesium alloys or composites based on carbon fibres. Therefore, they are widely used in aerospace and space constructions, but also in means of civil transport, including cars [1-3]. Aluminium and most of its wrought alloys are considered well weldable. However, when fusion welding aluminium there are a number of difficulties related to the ease of oxidation, oxide properties (high melting point, insoluble in liquid metal, non-wettable), high thermal conductivity, no colour change when heated and metallurgical properties. During electric resistance welding additionally the low electric resistance is another difficulty [4-6].
On the other hand, laser welding, as an advanced method with many advantages, is also increasingly used to join elements made of aluminium alloys. However, in this case there is one more significant difficulty related to the strong reflection of laser radiation from the aluminium surface. The reflection of the laser radiation is especially intense for the molecular CO_2 lasers emitting at the wavelength of 10.6 µm. Lower degree of reflection occurs in the case of lasers emitting a laser beam in a shorter wavelength range of about 1.0 µm or less. Therefore, near-infrared lasers are preferred for aluminium welding [1].
In the field of laser welding, many studies have been carried out, mainly focused on the influence of welding parameters on the quality of joints and mechanical parameters. The main problems during laser welding postulated by researchers concern also the wide range of temperature in vaporization and solidification which can lead to instability of the keyhole or blowholes, porosity and other defects such hot cracking or loss of alloying elements. The medium strength aluminium alloys of 5000 and 6000 series, characterised by relatively good technological properties, such as weldability or machinability, are the most widely used in industry. However, there is little information in the literature about keyhole laser welding of the series 5000 and 6000 aluminium alloys (Al-Mg-Si). In turn, authors of studies in this area indicate serious problems with ensuring the quality of joints, caused mainly by the tendency to create porosity and evaporation of alloy elements [2,4]. Most of the research concerns conduction mode of welding, because this mode is more stable due to significantly lower extend of metal evaporation [3,5]. Therefore, in this study the autogenous laser welding of butt joints of AlSi1MgMn aluminium alloy (6000 series) by a solid state disk laser was conducted. The influence of laser welding parameters, energy input on geometry, quality, microstructure, and microhardness distribution was investigated.

2. MATERIALS AND METHODOLOGY

The samples 200x100 mm in dimensions for laser welding tests were mechanically cut from a 3.0 mm thick sheet of AlSi1MgMn alloy at delivery conditions, Table 1 to Table 3.

Table 1. Chemical composition (wt.%) of the aluminium alloy AlSi1MgMn

Accor. to	Si	Mg	Mn	Fe	Cr	Zn	Ti	Cu	Al
EN*	0.7–1.3	0.6–1.2	0.4-1.0	< 0.5	< 0.25	< 0.2	< 0.1	< 0.1	Bal.
Tested	1.02	0.86	0.54	0.32	0.01	0.01	0.02	0.05	Bal.

Remarks: * - according to standard EN 573-1

Table 2. Physical properties of pure aluminium

Density g/cm^3	Melting point °C	Thermal expansion 1/K	Modulus of Elasticity GPa
2.7	555	24x10^{-6}	70

Table 3. Mechanical properties of the aluminium alloy AlSi1MgMn according to standard EN 485-2, 1.5÷3.0 mm

Tensile strength MPa	Yield point $Rp_{0.2}$	Elongation A_{50}, %	Hardness HB
150	85	16	40

Tests of welding were conducted by means of a fully automated and programmable stand with the solid state disk laser TruDisk 3302. The maximum output power of the laser was 3.3 kW, while the laser beam divergence angle 8.0 mm·mrad. At the applied configuration of the optics and the focusing head, the focal diameter was 200 µm, Figure 1.

In the initial phase of the study, bead-on-plate welding tests were performed in order to determine the lowest and the highest energy input for welding of butt joints, providing full penetration and proper shape of the weld, Table 4.

Prior to welding tests, the oxide layer was brushed and removed from the surface by means of a brass wire brush, and the surface of the sheet was degreased with 96% ethyl alcohol. Samples were clamped and stiffened mechanically. The flow of high purity argon (99.999%) by a cylindrical nozzle 8.0 mm in diameter was applied for protection of the weld region. The flow rate of argon was approx. 12÷15 l/min. Since the reflection of the laser radiation from the aluminum surface is high, the laser head was tilted at an angle of 12 degrees to avoid the risk of damage to the optics, Figure 1. The laser beam was focused on the top surface of the sheets to be welded.

Fig. 1. A view of bead-on-plate laser welding of aluminium alloy AlSi1MgMn by the TruDisk 3302 laser (head tilted at 12°)

Table 4. Parameters of autogenous laser welding of AlSi1MgMn butt joints of 3.0 mm thick sheets

Weld No.	Output laser power kW	Welding speed m/min	Energy input J/mm	Width of the weld face mm	Width of the weld root	Remarks
J1	2.0	1.5	80	2.1	2.7	FP, U
J2	2.5	2.0	75	2.6	3.1	FP,U

Remarks: FP – full penetration, U – uneven face

After making the test welded joints, the assessment of quality was made. The Quality Assessment was performed starting from visual inspections (VT) performed according to PN-EN 970 standard. Next samples were taken for metallographic study and cross-section observations.

The cross-sections were prepared by standard metallographic procedure. First, the samples were sanded with water sandpaper with a grit of 120 to 2500, next polished by diamond suspension of 3 µm. The microstructure was revealed by etching in 20% sodium hydroxide. Macrographs and micrographs were prepared for observation by light microscopy. Next the microhardness distribution across the joints was determined by Vickers tester according to PN-EN ISO 6507-1.
Mechanical properties of test joints were examined using the technological bending test (PN-EN ISO 5173-2010) and static tensile test (PN-EN 10045-1).

3. RESULTS AND DISCUSSION

In the first step, visual examinations VT and an initial quality assessment of the test joints were carried out. It was found that for each joint, a lack of full penetration was found in the initial length of about 15 to 20 mm. The width of the weld face increases gradually over this length until it reaches a stable value for the remaining length of the weld, as can be seen in Fig. 2. This phenomenon is caused by the stabilization of thermal conditions in the initial phase. This is mainly because of a high thermal conductivity of aluminium and also due to high reflectivity of the laser radiation. As a result, increase of the absorption and heat energy transferred to the substrate material is gradual (absorption depends also on the temperature). On the other hand, there is usually a small crater at the end of the weld, caused by a sudden shutdown of the laser beam or the laser beam exiting the joint area. At the same time, the properties of aluminium in the liquid state make the tendency to create craters and shrinkage cavities higher compared to steel. This is due to the physical properties, but also the casting shrinkage of aluminium at the level of approx. 6%.

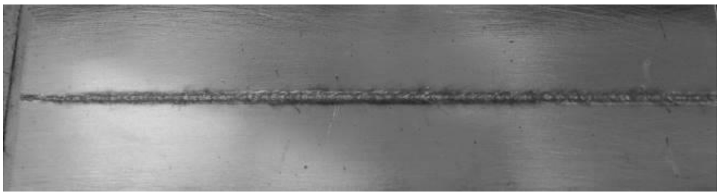

Fig. 2. A view of a representative test joints of AlSi1MgMn 3.0 mm thick and 200 mm long sheets made at the laser beam power of 2.0 kW and welding speed 1.5 m/min (energy input 80 J/mm)

The problems described above can be solved by using a programmable change of welding parameters, including laser beam power or applying run-on and run-off tabs for starting and ending the process. However, such solution is an additional difficulty in the automated process. As can be seen on the representative joint, the surface of the weld face is not even and not smooth. There are irregular and uneven scales on the weld face. Such phenomenon occurs usually at high welding speed.
The average width of the face of welds made with higher energy input (80 J/mm) was 2.7 mm, and the root width was 2.1 mm. In turn, the weld face of joints produced at lower energy input (analytical value, heat transfer efficiency not considered) was higher approx. 3.1 mm and the root width was 2.6 mm. It should be emphasized, that aluminium is a characteristic material due to the significant reflection of the laser beam and, at the same time, high thermal conductivity, which makes it difficult to stabilize thermal conditions and heat flow during welding. For this reason, the degree of radiation absorption, and thus the amount of heat generated and transferred to the material, the amount of heat energy used to melt the material also depends on the welding speed and power density of the laser beam. That is why the energy input cannot be compared directly, under the conditions of the laser welding experiment. When the laser beam output power is increased, the efficiency of energy transfer and the degree of absorption are likely to be higher.
The mechanical properties of the test joints were determined using a technological bending test and a static tensile test. The configuration (arrangement) of the device for bending tests is shown in Figure 3.

Fig. 3. A view of the device for technological bending test of 3.0 mm thick butt joints of AlSi1MgMn and its configuration

a) b)

Fig. 4. A view of the samples of the butt test joint of AlSi1MgMn 3.0 mm thick sheets made at the energy input of 80 J/mm; a) after weld face bending (crack at approx. 100°), b) after root bending (full angle 180°)

Figure 4 shows representative samples of just one test joint after bending tests. However, in the case of all tested joints, the results were convergent. Each sample testes under bending from the root side obtained positive results of the bending angle of 180°. In turn, the samples bent from the weld face side cracked at the bend angle 90÷100°. Such a result may suggest that defects accumulate near the weld face or there are discontinuities in this weld region.

Static tensile tests were carried out in accordance with the PN-EN 10045-1 standard, Figure 5.

The results of the static tensile test are consistent for all tested joints, Figures 6, 7, Table 5. The differences result rather from the measurement error and it is not possible to conclude about any dependence related to the welding parameters. However, all the test joints fracture in weld region, indicating softening of weld metal. The average tensile strength of the joints is ranged within 201÷221 MPa, Table 5.

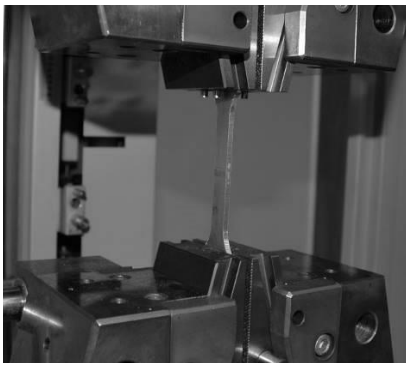

Fig. 5. A view of the static tensile tests of samples prepared according to PN-EN 10045-1

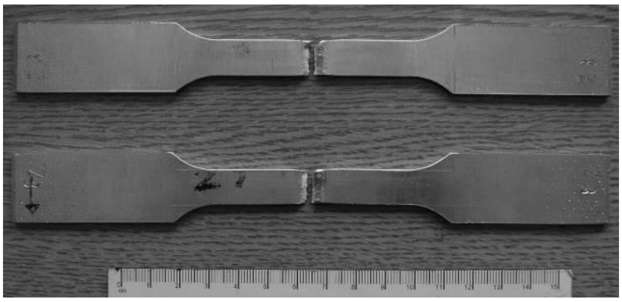

Fig. 6. A view of the representative samples of the butt test joint of AlSi1MgMn 3.0 mm thick sheets made at the energy input of 80 J/mm after static tensile tests

Table 5. Results of static tensile tests of 3.0 mm thick joints of AlSi1MgMn aluminium alloy

Joint	Sample No.	Fracture force, kN	Tensile strength MPa	Fracture region
J1	J1_1	7.96	221.2	Fusion zone
	J1_2	7.87	218.8	Fusion zone
J2	J2_1	7.25	201.5	Fusion zone
	J2_2	7.52	208.8	Fusion zone

The exemplary tensile diagrams indicate that the yield range of the material is narrow. However, welded joint is not homogeneous material. This type of tensile curve is characteristic in the case of fracturing samples in the weld metal. It is also worth noting that the tensile strength of the joints is higher than the minimum required for the material according to the standard within the thickness range (150 MPa for 3.0 mm thick plate).

Next, metallographic examinations were carried out, starting with macroscopic observations. The macrographs of cross-sections of test joints are shown in Figure 8. As can see in the macrographs, the fusion line is clear, while the heat affected zone (HAZ) is very narrow. The width of the HAZ is roughly estimated to be no more than 0.2÷0.3 mm. This is due to the high thermal conductivity of aluminium.

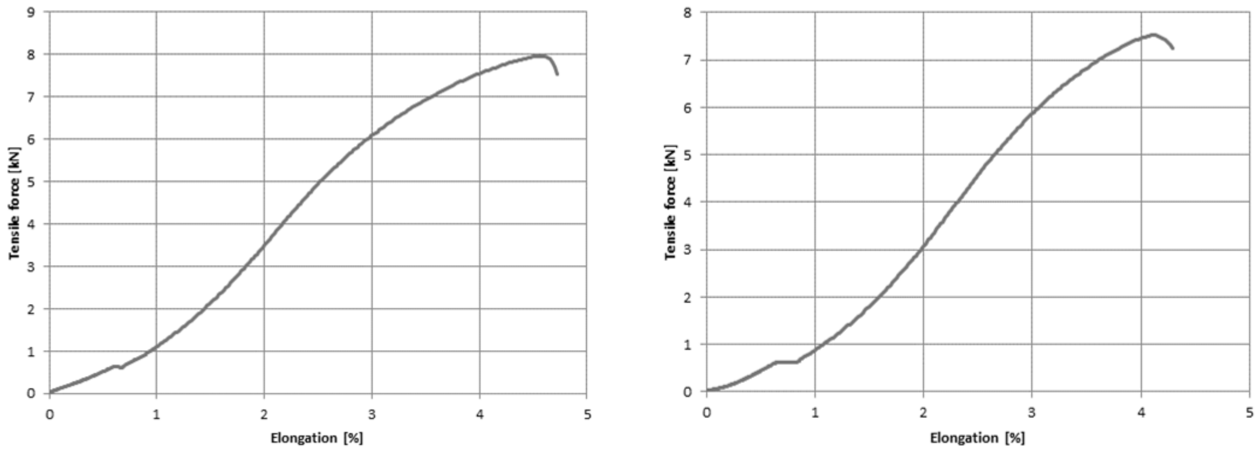

a) b)

Fig. 7. Tension curves for representative test joints: a) J1 produced at energy input 80 J/mm, b) J2 produced at energy input 75 J/mm

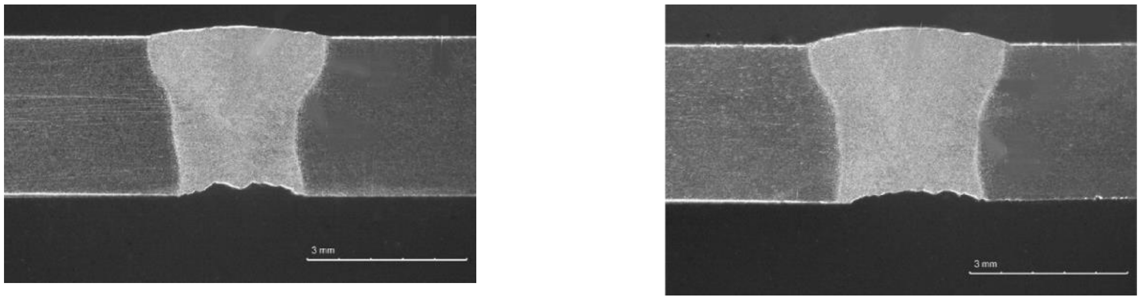

a) b)

Fig. 8. Macrostructure of 3.0 mm thick joints of AlSi1MgMn aluminium alloy: a) J1 produced at energy input 80 J/mm, b) J2 produced at energy input 75 J/mm

In each case, slight weld face reinforcement and a concavity of the root are also clearly visible. The concavity of the root does not exceed 0.3 mm. However, no internal defects such as porosity, cracks, inclusions or discontinuities were found. The shape of the fusion zone (weld) is columnar, with a width smaller or comparable to the depth of fusion (penetration), which indicates a welding mechanism not typical for a keyhole mode, but rather between conductive and keyhole mode welding.

Measurements of the microhardness distribution on the cross-section of the joints were made with a load of 100 g. The distance between successive measurement points was 0.5 mm. In turn, for each joint, measurements were made in two lines, the first at a distance of 0.5 mm from the upper surface (face side) and the second at a distance of 0.5 mm from the lower surface of the sheets (root side), Figure 9.

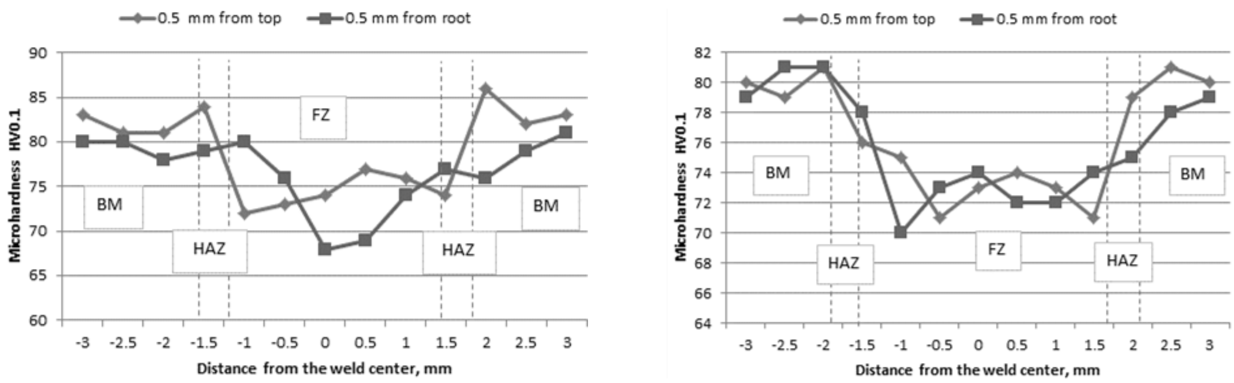

a) b)

Fig. 9. Microhardness distribution across the test butt joints of 3.0 mm thick AlSi1MgMn aluminium alloy sheets: a) J1 produced at energy input 80 J/mm, b) J2 produced at energy input 75 J/mm

The results indicate that the microhardness of the base metal is approx. 80-84 $HV_{0.1}$, Figure 9. In the fusion zone, there is a rapid drop in microhardness to approx. 70-74 $HV_{0.1}$. At the same time, the zone in which there is a rapid

change in microhardness between the base metal and the fusion zone is narrow and does not exceed two successive measurement points (0.5 mm).
Microstructure of the interface region and fusion zone of the comparative test joints is presented in Fig. 10. As can be seen in Figure 10, the fusion zone is clear as well as the interface between base metal and fusion zone. The microstructure of the base material is typical for the plate after rolling, as fine-grained elongated grains are visible along the longitudinal axis, i.e. the direction of rolling. Numerous precipitates in the microstructure of the base metal (black spots) are also characteristic due to the chemical composition of the aluminium alloy containing significant amounts of alloying elements.
The as-delivered sheets were probably supersaturated after rolling or during the rolling process as a thermomechanical treatment to ensure high mechanical properties, hardness and strength. The mentioned precipitate areas observed in the microstructure of the base metal are probably precipitates containing Mg and Si, most likely intermetallic phases Mg_2Si.
Partially melted crystals can be identified in this region. Next the narrow zone of equiaxed grains that grew on the partially melted crystals. Entire width of the mentioned above zone does not exceed 50 μm. Next, the columnar dendritic growth zone with a privileged crystallographic orientation at the initial stage can be seen. Microstructure of the middle region of the comparative fusion zones of the joints is shown in Figure 11.

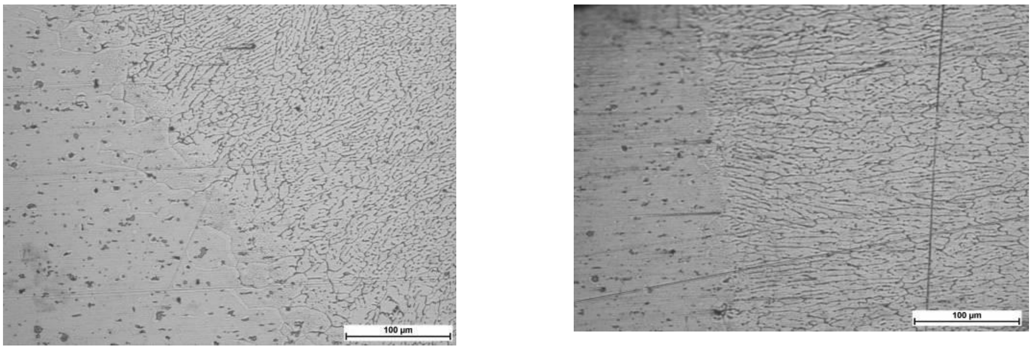

a) b)

Fig. 10. Comparative microstructure of test joints of AlSi1MgMn aluminium alloy in fusion line vicinity: a) J1 produced at energy input 80 J/mm, b) J2 produced at energy input 75 J/mm

The main difference in the microstructure is the presence of equiaxed crystals in the middle region. As can be seen, the grain size for the weld produced at lower energy input is also lower. However, quantitative analysis was not performed for comparison the grain size. A comprehensive analysis requires taking into account different zones of the weld. On the other hand, the difference in energy input seems to be not significant for providing significant changes in microstructure of the welds. Additionally, it can be noticed that the interdendritic regions in fusion zone also contains precipitations of second phases in the solid solution of aluminium matrix Figure 11. These precipitates are most likely intermetallic phases formed as a result of lowering the solubility of the alloying elements in the aluminium solution during cooling. Such precipitates usually contain Al, Fe, Mn and Si and also Mg_2Si. One of the reasons for the decrease in hardness as a result of aging of the AlSi1MgMn alloy is the decrease in the content of Mg and Si in the solution and also uneven distribution of reinforcing precipitates in the structure.

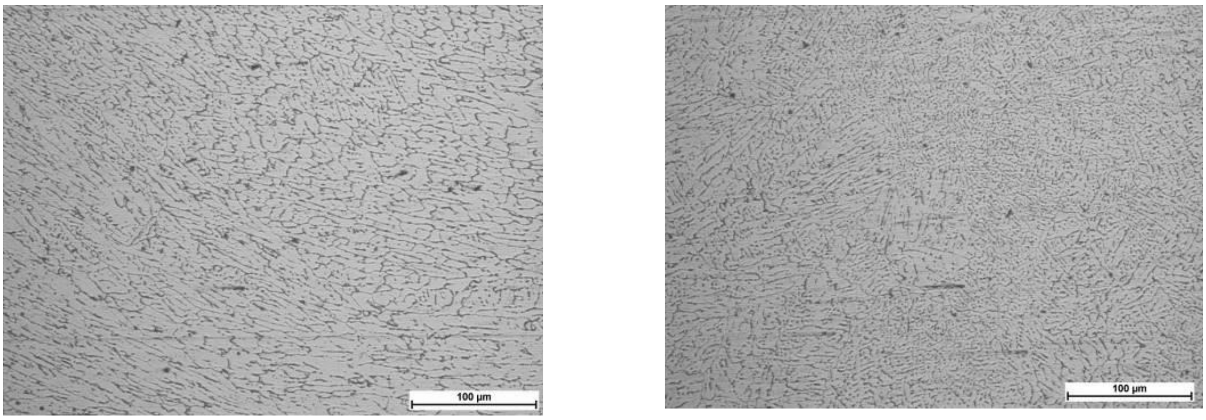

a) b)

Fig. 11. Comparative microstructure of test joints of AlSi1MgMn aluminium alloy in middle region of fusion zone: a) J1 produced at energy input 80 J/mm, b) J2 produced at energy input 75 J/mm

Analysing the microstructure on the cross-section of the joints and taking into account the decrease in hardness in the fusion zone, the main factors responsible for this decrease can be identified. This phenomenon is caused by a decrease in the degree of supersaturation of the Al solution, uneven distribution of strengthening intermetallic phases in the interdendritic spaces and, additionally, an increase in grain size in this zone.

4. CONCLUSIONS

The following conclusion have been drown based on the study of autogenous laser welding 3.0 mm thick AlSi1MgMn aluminium alloy sheets at butt configuration with a disk laser:
1) Under the conditions of the experiment, full penetration of 3.0 mm thick sheets and acceptable quality of joints were provided at energy input 75÷80 J/m and relatively high welding speed 1.5÷2.0 m/min. However, the window of optimal parameters is extremally narrow during laser welding of this aluminium alloy. Slight deviations in parameters caused instability of welding process resulted in local burnouts or lack of fusion. Material properties play a significant role in the heating mechanism, energy transfer, and thermal efficiency and weld formation.
2) The weld metal of all tested joints was characterised by a proper geometry of fusion zone and now internal imperfections. Mechanical properties were satisfactory however, the toughness and tensile strength was reduced. Fracture zone during tensile tests was placed in fusion zone. Samples tested under bending test showed full angle without crack whet the root side was bended. In turn, when weld face side was bended the angle was clearly reduced to 90÷100°. This phenomenon is mainly due to the shape of the face and root (stress concentration), rather than metallurgical features.
3) The weakening of the joint in the weld results from a decrease in hardness and microstructure. The microstructure of the base metal was approx. 80-84 $HV_{0.1}$, while a clear decrease in fusion zone was observed to approx. 70-74 $HV_{0.1}$.
4) Three main factors responsible for hardness decrease have been identified. The first is reducing the degree of supersaturation of aluminium solutions by alloying elements (Al, Fe, Mn, Si, Mg). The second is uneven distribution of strengthening intermetallic phases in the interdimeric spaces, e.g. Mg_2Si. Finally, the grain growth in fusion zone determines the properties and hardness of this zone.

ACKNOWLEDGEMENTS

The study was carried out under a grant 10/050/SDU/10-21-01.

5. REFERENCES

1. Zhou, J., Xia, G., Zhou, Z., Chen, C., Long, Y., (2023). *Comparison study of 6082 Al alloy laser welding using 455 nm blue laser and 1080 nm near-infrared laser*. Optik 272, 170224.
2. Yuce, C., Tutar, M., Karpat, F., Yavuz, N., Tekin, G., (2017). *The Effect of Process Parameters on the Microstructure and Mechanical Performance of Fiber Laser-Welded AA5182 Aluminium Alloys*. Strojniški vestnik - Journal of Mechanical Engineering 63, 9, 510-518.
3. Sanchez-Amaya, J.M., Delgado, T., Gonzalez-Rovira, L., Botana, F.J., (2009). *Laser welding of aluminium alloys 5083 and 6082 under conduction regime*. Applied Surface Science, 255, 9512–9521.
4. Kurc-Lisiecka, A., Lisiecki, A. (2017). *Laser welding of new grade of advanced high strength steel Domex 960,* Mater. Technol., 51, 199–204.
5. Lisiecki, A., Kurc-Lisiecka, A., (2018). *Automated laser welding of AISI 304 stainless steel by disk laser*, Arch. Metall. Mater., 63, 4, 1663-1672.
6. Landowski, M., Świerczyńska, A., Rogalski, G., Fydrych, D., (2020). *Autogenous Fiber Laser Welding of 316L Austenitic and 2304 Lean Duplex Stainless Steels*. Materials, 13, 2930.

Received: August 22, 2023 / Accepted: December 15, 2023 / Paper available online: December 20, 2023 © International Journal of Modern Manufacturing Technologies